journal

J. Am. Ceram. Soc., 75 [9] 2610–12 (1992)

In-Situ Alumina/Aluminate Platelet Composites

Pei-Lin Chen* and I-Wei Chen*

Department of Materials Science and Engineering, University of Michigan, Ann Arbor, Michigan 48109-2136

Alumina composites containing in-situ-formed hexaaluminate ($LaAl_{11}O_{18}$, $LaMgAl_{11}O_{19}$, $SrAl_{12}O_{19}$, and $Mg_2NaAl_{15}O_{25}$) platelets can be pressureless-sintered to high density. The grain morphology of the aluminates can be controlled by composition. A peak toughness 50% higher than that of alumina is obtained at 30 vol% aluminates, with a modest reduction (10%) in hardness and Young's modulus. Although crack-bridging by aluminate platelets is apparently operating, the maximum toughness is intrinsically limited by the low cohesive strength of these layer compounds.

I. Introduction

In the last decade ceramists have pursued microstructural toughening through use of a second phase with a high aspect ratio (whiskers, fibers, and platelets). These composites are difficult to sinter to high density, however, because of the constraint of the second-phase network, and they must be hot-pressed in most cases. Ideally, if the microstructural features are developed after densification is first completed, via in-situ formation of a second phase which has a highly anisotropic growth habit, then a tough ceramic composite can be obtained without the sintering difficulty. For example, Hori *et al.*[1] reported an in-situ composite of TiO_2 matrix with dispersed corundum platelets whose anisotropic growth was promoted by sodium doping. Toughness of up to 7 $MPa \cdot m^{1/2}$ was obtained. In another case, in-situ formation of elongated, rodlike grains in Si_3N_4 sintered under a nitrogen-gas overpressure, resulted in self-reinforcement with an improved toughness in excess of 10 $MPa \cdot m^{1/2}$.[2] In both examples, high density could readily be achieved. Successful toughness enhancement was also reported for 3Y-TZP/mullite composites in which elongated mullite grains could be formed in situ,[3] although much of the mullite effect, in our opinion, seemed to be attributable to the larger grain size in the composite which facilitates transformation toughening.

To adopt the above alloy development concept for use in the Al_2O_3 system, we first searched for a compatible second phase with an anisotropic growth habit. Al_2O_3 is compatible with many layer aluminate compounds such as $LaAl_{11}O_{18}$ (with β-alumina structure) and $LaMgAl_{11}O_{19}$ (with magnetoplumbite structure), as well as others in the same structural family. These aluminates may be termed hexaluminates in analogy to the similar structural family of hexaferrite. They are composed of spinel blocks separated by layers of cations and oxygen ions. Such compounds are highly stable and anisotropic, and may be well suited for toughening reinforcements. Indeed, by incorporating these phases into transformation-toughened ZrO_2, favorable results have been reported. Tsukuma and Takahata added a small amount of La_2O_3 to 2Y-TZP/Al_2O_3 to form $LaAl_{11}O_{18}$ platelets.[4] The resultant composite had a higher fracture toughness and higher strength at high temperatures as compared to the base 2Y-TZP/Al_2O_3. Cutler *et al.*[5] used SrO as the additive in forming in-situ platelets of $SrAl_{12}O_{19}$ in Ce-TZP to obtain an attractive combination of high levels of strength, toughness, and hardness. The present report is an account of the Al_2O_3/($LaAl_{11}O_{18}$, $LaMgAl_{11}O_{19}$, $SrAl_{12}O_{19}$, $Mg_2NaAl_{15}O_{25}$) system in which the benefits and limitations of in-situ-formed aluminate platelet composites are examined.

II. Experimental Procedure

(1) Composition

Al_2O_3, $LaAl_{11}O_{18}$, and $LaMgAl_{11}O_{19}$ form a compatibility triangle which we systematically investigated, especially along the $Al_2O_3/LaAl_{11}O_{18}$ and the $Al_2O_3/LaMgAl_{11}O_{19}$ binaries. MgO at 0.1 wt% was added as a sintering aid to nearly all the specimens in this group. In an attempt to control phase morphology and/or size, as well as their interface characteristics, dopants at 1 wt% were added to 70 vol% Al_2O_3/30 vol% $LaAl_{11}O_{18}$. These dopants were chosen to cover a range of ionic charge and size or to provide a glassy liquid. They included Li^+, Na^+, Mn^{2+}, Sr^{2+}, Sc^{3+}, Y^{3+}, Zr^{4+}, and Si^{4+}, some in pairs. Additionally, the composites of Al_2O_3 and two other aluminates ($NaMg_2Al_{15}O_{25}$ and $SrAl_{12}O_{19}$) at 30 vol% were investigated.

(2) Sample Preparation and Testing Procedure

Commercially available high-purity (>99.99%) Al_2O_3 powder (AKP-50, Sumitomo Chemical America), and nitrate or carbonate powders were used as starting materials. SiO_2 and ZrO_2 in the form of oxides were directly used. The nitrate or carbonate powders were dissolved in water or acid, then added to a well-dispersed Al_2O_3 slurry, and the pH of the mixture was adjusted to prevent flocculation. The slurry was dried, and powders were obtained after calcination at 750°C for 2 h. The calcined powders were dispersed by attrition milling before casting into cakes by pressure filtration. The dried cakes were isostatically pressed and sintered in air from 1550° to 1650°C for times up to 3 h.

The density of the sintered materials was determined by the water displacement method. Microstructural examination and phase identification were performed by standard scanning electron microscopy (SEM) and X-ray diffraction (XRD) methods. Grain sizes were determined using the average linear intercept length of at least 500 grains. Hardness and fracture toughness were measured by using a Vickers diamond indenter in a universal hardness-testing machine. In addition, average elastic constants were measured by a pulse–echo technique using ultrasound.

III. Results and Discussion

All the samples prepared in this study, including the aluminates themselves and composites of various phase assemblages, were better than 99% of their theoretical density. The phases identified by XRD are corundum for Al_2O_3, β-Al_2O_3 for $LaAl_{11}O_{18}$, magnetoplumbite for $LaMgAl_{11}O_{19}$, and $SrAl_{12}O_{19}$

D. K. Shetty—contributing editor

Manuscript No. 196026. Received January 29, 1992; approved June 17, 1992.
Presented at the 93rd Annual Meeting of the American Ceramic Society, Cincinnati, OH, May 2, 1991 (Ceramic Matrix Composites Symposium, Paper No. 111-SVI-91).
Supported by the U.S. Department of Energy (BES) under Grant No. DE-FG02-87ER45302.
*Member, American Ceramic Society.

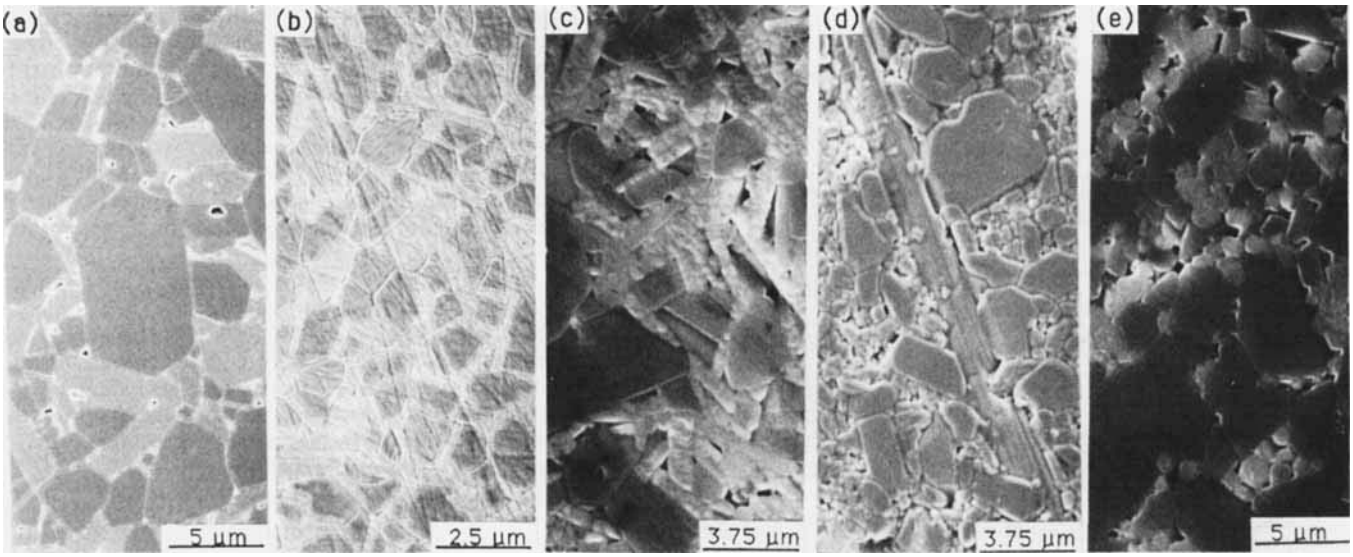

Fig. 1. Microstructures of composites (30 vol% aluminate/70 vol% Al_2O_3): (a) $LaAl_{11}O_{18}$, (b) $LaMgAl_{11}O_{19}$, (c) $SrAl_{11}O_{19}$, (d) $Mg_2NaAl_{15}O_{25}$, and (e) MgO–SiO_2–Na_2O-doped 30 vol% $LaAl_{11}O_{18}$/70 vol% Al_2O_3.

and β‴-Al_2O_3 for $Mg_2NaAl_{15}O_{25}$, as predicted from their compositions and phase relations.

Generally, the aspect ratio of aluminates increases in the following order: $LaAl_{11}O_{18}$, $LaMgAl_{11}O_{19}$, $SrAl_{12}O_{19}$, and $Mg_2NaAl_{15}O_{25}$. This is shown in Figs. 1(a) to (d) which compare microstructures of four composites with 30% aluminate phase each. (The aluminate appears as the whiter phase in Figs. 1(a) to (c) and is due to the heavy element lanthanum or strontium. It has little contrast in Fig. 1(d) but can be easily recognized by its elongated shape.) In the case of $LaAl_{11}O_{18}$, we further found that the aspect ratio and the particle size were dopant dependent. When Mg, Sr–Mg, Sc–Mg, Y–Mg, Sr–Mg, and Zr–Mg were used, elongated aluminate grains were found. However, when dopants Mn–Mg, Li–Mg, Li–Si–Mg, and Na–Si–Mg were added, aluminate grains became more equiaxed, as shown in Fig. 1(e). In general, as the amount of the phase (either Al_2O_3 or aluminate) decreases, its grain size (or particle size) and aspect ratio decrease. This microstructure refinement is less drastic for Al_2O_3 than for aluminates. For $LaAl_{11}O_{18}$ and $LaMgAl_{11}O_{19}$, a minimum of about ~25 vol% is required for the development of an elongated morphology. This requirement is probably due to phase connectivity consideration and is apparently less stringent for $NaMg_2Al_{15}O_{25}$, which forms high-aspect-ratio platelets even at low volume fractions.

Hardness and Young's modulus of aluminates is much lower than that of corundum, and the composite properties follow a monotonic trend. This is shown in Fig. 2 for the Al_2O_3/$LaAl_{11}O_{18}$ binary. The difference in these properties is ~45% between end members.

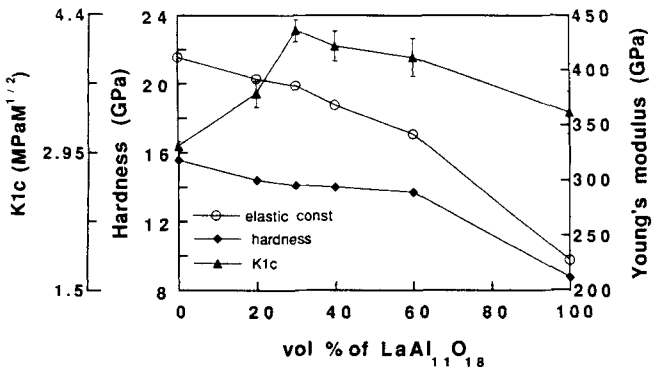

Fig. 2. Hardness, Young's modulus, and fracture toughness versus volume fraction of $LaAl_{11}O_{18}$ in MgO-doped Al_2O_3/$LaAl_{11}O_{18}$ composites.

Despite their lower hardness and Young's modulus, the aluminates have a slightly higher toughness than corundum. Moreover, the fracture toughness of the composites reaches a peak at an intermediate aluminate fraction of 30 vol%, as shown in Fig. 2. The increment of the toughness over the base line between end members is about 40%, or 50% if compared with the toughness of Al_2O_3. We have not found much difference between various composites regarding the toughness values at this volume fraction. For example, $LaMgAl_{11}O_{19}$ has a Young's modulus of 215.4 GPa, a hardness of 8.5 GPa, and a toughness of 3.2 MPa·$m^{1/2}$; its composite at 30 vol% has a toughness of 4.3 MPa·$m^{1/2}$. At the latter volume fraction, the toughness values measured for other composites are 4.4 MPa·$m^{1/2}$ for $SrAl_{12}O_{19}$ and 4.5 MPa·$m^{1/2}$ for $Mg_2NaAl_{15}O_{25}$.

Fractography in Fig. 3(a) reveals that, at peak toughness, a crack propagates through Al_2O_3 grains (A), aluminate platelets (B), along Al_2O_3 grain boundaries (C), and along phase interfaces (D). At a higher volume fraction of aluminates, crack bridging by aluminate ligaments was quite frequently observed, but transgranular fracture was rare. The comparison is shown in Fig. 3.

The toughness increase cannot be due to the variation of the corundum grain size, which decreases monotonically with the addition of aluminates. Indeed, it is well documented that the toughness of Al_2O_3 increases with increasing grain size up to a critical grain size, which is beyond the range of this study. Thus, it seems reasonable to attribute the toughening effect to crack-bridging processes similar to those observed in SiC-whisker-reinforced Al_2O_3. The increased toughness in our case, however, is modest compared to that reported for SiC-whisker reinforcement, for which a peak toughness of up to 9 MPa·$m^{1/2}$ at 30 vol% has been reported.[6]

Toughening by whisker reinforcements can be expressed by the energy dissipation ΔJ as

$$\Delta J = Vr\sigma_f^3/6E\tau \quad (1)$$

where V is the volume fraction of the whisker, r the whisker radius, σ_f the whisker fracture stress, E the Young's modulus of the whisker, and τ the interfacial friction between whisker and matrix.[6] This result is based on the assumption that the interface toughness is low enough to allow the whisker to debond at the crack tip and that load is gradually transferred to the bridging

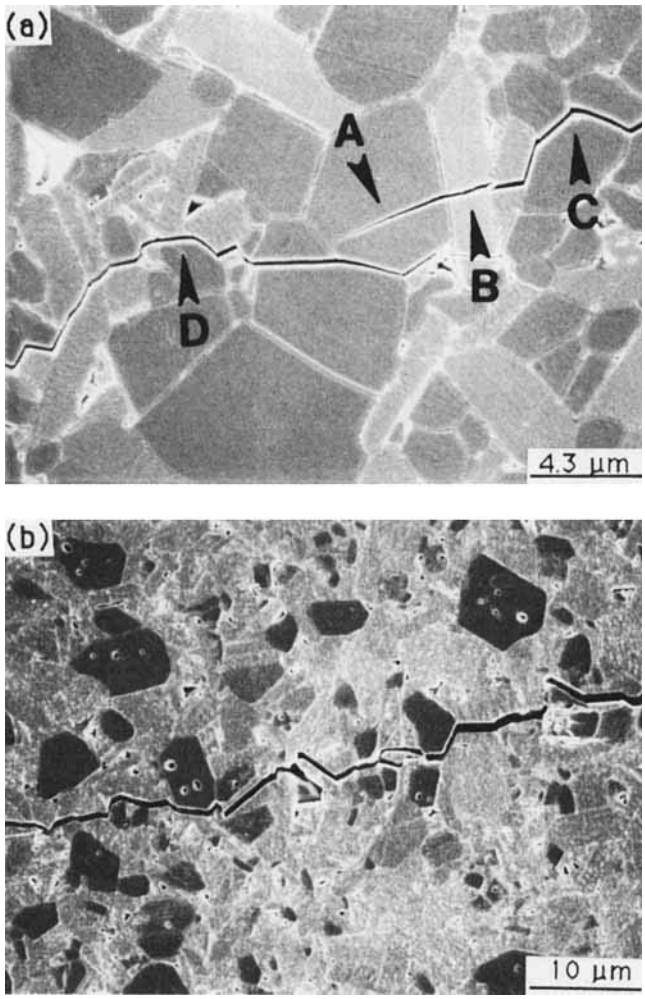

Fig. 3. Fracture microstructures of MgO-doped $LaAl_{11}O_{18}/Al_2O_3$: (a) 30 vol% $LaAl_{11}O_{18}$ and (b) 60 vol% $LaAl_{11}O_{18}$.

whiskers in the wake by friction across the whisker interface. Evidently, high-aspect-ratio aluminate platelets partially fulfill the prerequisites for a potent reinforcement by having a relatively large grain radius and a very low elastic modulus. The interface toughness also seems sufficiently low, as suggested by the frequent observations of interface debonding. In our study, more favorable interface characteristics (low roughness and friction) most likely were present given the large variety of phases, dopants, and morphologies investigated. Nevertheless, only a relatively modest energy dissipation was witnessed in all the composites prepared. We believe the reason for their failing lies in the inherently low cohesive strength of hexaluminates, which is traced to their atomic structures because of the weak bonding between spinel blocks as a result of the large spacing and few bonds therein. The latter is presumably also responsible for the low Young's modulus and hardness. (The aluminates can be considered self-reinforced by their characteristic interlocking platelike grains, resulting in the relatively high toughness of ~3.2 $MPa \cdot m^{1/2}$.)

Although the layer spacing and bonding are conceivably amenable to modification by judicious tailoring using crystal chemistry means, our exploration of four aluminates in this family unfortunately failed to yield further improvement in toughness despite the difference in their phase morphology. We should also mention that, at the same time this paper was presented, two other investigations on $Al_2O_3/NaMg_2Al_{15}O_{25}$ composites were reporting essentially the same toughness value.[7,8] The limit of aluminate platelet toughening thus seems quite evident.

In retrospect, it is now clear that the strength and hardness improvement reported for aluminate-modified Ce-TZP could not be due to platelet reinforcement.[5] Rather, the benefit is from the interruption of ZrO_2-phase connectivity which leads to suppression of autocatalytic transformation.[9] This example suggests that, although aluminates are not particularly strong and tough, they might still be advantageously exploited in ceramic composite design under suitable conditions.

IV. Conclusions

A variety of in-situ Al_2O_3/aluminate composites have been explored with the following results:

(1) The composites can all be sintered to high density.

(2) Aluminates develop in situ a platelet morphology whose aspect ratio is dependent on the major and minor composition and the phase fraction; very elongated grains can be obtained readily in some cases.

(3) The composites exhibit a peak toughness of around 4.3 $MPa \cdot m^{1/2}$ at 30 vol% aluminates, representing a 50% increase over that of Al_2O_3 with only a modest reduction (10%) of hardness and Young's modulus.

(4) The composites and the aluminates themselves can be considered toughened by the crack-bridging action of the aluminate platelets; however, the intrinsically low cohesive strength of these layer compounds limits the maximum toughness derivable from their reinforcement.

References

[1]S. Hori, H. Kaji, M. Yoshimura, and S. Sōmiya, "Deflection-Toughened Corundum–Rutile Composites," *Mater. Res. Soc. Symp. Proc.*, **78,** 283–88 (1987).

[2]E. Tani, S. Umebayashi, K. Kishi, and M. Nishijima, "Gas-Pressure Sintering of Si_3N_4 with Concurrent Addition of Al_2O_3 and 5 wt% Rare-Earth Oxide: High Fracture Toughness Si_3N_4 with Fiberlike Structure," *Am. Ceram. Soc. Bull.*, **65** [9] 1311 (1986).

[3]K. Okada, N. Otsuka, R. J. Brook, and A. J. Moulsob, "Microstructure and Fracture Toughness of Yttria-Doped Tetragonal Zirconia Polycrystal/Mullite Composites Prepared by an in Situ Method," *J. Am. Ceram. Soc.*, **72** [12] 2369–72 (1989).

[4]K. Tsukuma and T. Takahata, "Mechanical Property and Microstructure of TZP and TZP/Al_2O_3 Composites," *Mater. Res. Soc. Symp. Proc.*, **78,** 123–35 (1987).

[5]R. A. Cutler, R. J. Mayhew, K. M. Prettyman, and A. V. Virkar, "High-Toughness Ce-TZP/Al_2O_3 Ceramics with Improved Hardness and Strength," *J. Am. Ceram. Soc.*, **74** [1] 179–86 (1991).

[6]P. F. Becher, "Microstructural Design of Toughened Ceramics," *J. Am. Ceram. Soc.*, **74** [2] 255–69 (1991).

[7]P. E. Morgan, D. B. Marshall, and J. R. Porter, "Reactive Approaches to Interface Forming in Ceramic/Ceramic Composites"; presented at the 93rd Annual Meeting of the American Ceramic Society, Cincinnati, OH, April 30, 1991 (Ceramic Matrix Composites Symposium, Paper No. 56-SVI-91).

[8]I. S. Lee, J. W. Ko, S. Y. Lee, and H. D. Kim, "Alumina Ceramics Reinforced with Needle-Shaped β‴-Alumina"; see Ref. 7, Paper No. 9-SVIP-91.

[9]P. E. Reyes-Morel and I-W. Chen, "Transformation Plasticity of CeO_2-Stabilized Tetragonal Zirconia Polycrystals: I, Stress Assistance and Autocatalysis," *J. Am. Ceram. Soc.*, **71** [5] 343–53 (1988). □